OPTIMISATION OF PHOTON-SAIL TRAJECTORIES IN THE ALPHA-CENTAURI SYSTEM USING EVOLUTIONARY NEUROCONTROL

Frederic Schoutetens[1,4], **Prof. Dr. Bernd Dachwald**[2], **Dr. Jeannette Heiligers**[3]

[1] *Graduate Student, Faculty of Aerospace Engineering, Delft University of Technology, Kluyverweg 1, 2629 HS Delft, the Netherlands, +49 151 40368746, frederic.schoutetens@community.isunet.edu*
[2] *Professor, Faculty of Aerospace Engineering, FH Aachen University of Applied Sciences, Hohenstaufenallee 6, 52064 Aachen, Germany, +49 241 6009 52343, dachwald@fh-aachen.de*
[3] *Assistant Professor, Faculty of Aerospace Engineering, Delft University of Technology, Kluyverweg 1, 2629 HS Delft, the Netherlands, +31 15 27 86221, M.J.Heiligers@tudelft.nl*
[4] *Flight Dynamics Engineer, German Space Operations Center, DLR, Münchener Str. 20, 82234 Weßling, Germany, +49 8153 282269, frederic.schoutetens@dlr.de*

ABSTRACT

With the increased interest for interstellar exploration after the discovery of exoplanets and the proposal by Breakthrough Starshot, this paper investigates the optimisation of photon-sail trajectories in Alpha Centauri. The prime objective is to find the optimal steering strategy for a photonic sail to get captured around one of the stars after a minimum-time transfer from Earth. By extending the idea of the Breakthrough Starshot project with a deceleration phase upon arrival, the mission's scientific yield will be increased. As a secondary objective, transfer trajectories between the stars and orbit-raising manoeuvres to explore the habitable zones of the stars are investigated. All trajectories are optimised for minimum time of flight using the trajectory optimisation software InTrance. Depending on the sail technology, interstellar travel times of 77.6 - 18,790 years can be achieved, which presents an average improvement of 30% with respect to previous work. Still, significant technological development is required to reach and be captured in the Alpha-Centauri system in less than a century. Therefore, a fly-through mission arguably remains the only option for a first exploratory mission to Alpha Centauri, but the enticing results obtained in this work provide perspective for future long-residence missions to our closest neighbouring star system.

1 INTRODUCTION

At 153 astronomical units (AU) away from the Sun and at a velocity of less than 0.01 AU/day, it would take Voyager 1 approximately 75,000 years to reach Alpha Centauri, the closest star system from Earth at approximately 275,000 AU. Due to its "close proximity" to Earth, Alpha Centauri is often considered the prime target for a future interstellar exploration mission [1]. It holds significant scientific importance for better understanding our Sun, and stars in general, and for advancing our knowledge on the formation and evolution of star systems [2]. Moreover, by visiting Alpha Centauri, Earth-like exoplanets may be discovered (in addition to the discovery of Proxima Centauri b in 2016). A photon-sail propelled spacecraft could surpass conventional methods of spacecraft propulsion in terms of travel time to Alpha Centauri by exclusively making use of the radiation pressure from a star as a means to drive the spacecraft forward. This novel propulsion technology has made significant technological progress through JAXA's IKAROS mission [3] - the first interplanetary solar-sail

mission - followed by NASA's NanoSail-D2 mission [4] and The Planetary Society's LightSail-1 and LightSail-2 missions [5, 6].

Initiatives with clear goals of reaching Alpha Centauri using photon-sail propulsion are already underway, in particular the Breakthrough Starshot project[1]. The proposed mission is a so-called "fly-through" mission, with a velocity of the spacecraft of 20% of the speed of light or approximately 35 AU/day, such that it will travel through Alpha Centauri's binary-star system in approximately one day. To increase the amount of time spent inside the Alpha-Centauri system and consequently increase the scientific return of the mission, this paper investigates photon-sail trajectories that allow the spacecraft to be captured around either of the stars, Alpha Centauri A or B. Research about the dynamics of a photon sail in a multi-star system such as Alpha Centauri is limited. Note that, due to the presence of two radiative sources, the dynamical model and resulting trajectories are unlike those in our own Solar System. To date, results for photon-sail trajectory optimisation in Alpha Centauri were obtained in [7, 8], assuming a graphene-based sail covered with a highly reflective coating. To decelerate upon arrival in Alpha Centauri, travel times of 75 years and maximum arrival speeds of 5.7% of the speed of light were obtained. Note that these results are obtained focusing on arrival at Proxima Centauri, while this current paper is focused on capture around the Alpha Centauri's binary system. The MIRA Collaboration focused on the computation of artificial equilibria (AE) in Alpha Centauri for a solar balloon spacecraft, before investigating capture and transfer trajectories in the elliptical restricted three-body problem (ER3BP) [2, 9]. The dynamics, stability and manoeuvrability of a photon-sail in a two-radiative ER3BP such as that of the Alpha Centauri system is further investigated in [10]. In the cited paper, the photon-sail artificial equilibria in the ER3BP under the effect of two radiative sources were obtained after a new photon-sail acceleration model for both a one-sided and two-sided reflective photon sail were derived that holds under the two-radiative source dynamics. The current paper uses the dynamical model derived in [10] and explores the optimisation of photon-sail trajectories in Alpha Centauri. Hence, the prime objective is to find the optimal steering strategy for a photonic sail to get captured into the Alpha-Centauri system after a minimum-time transfer from Earth. In particular, capture into a circular orbit at the centre of the habitable zone of one of the stars will be sought for. As a secondary objective, transfer trajectories between the stars and orbit-raising manoeuvres around either of the stars to explore the habitable zones of the stars are investigated. This secondary objective adds to the novelty of the paper by allowing for long-residence missions. Another novelty of this paper includes the trajectory optimisation software. All trajectories are optimised for minimum time of flight using the InTrance, a global low-thrust trajectory optimisation software using evolutionary neurocontrol [11, 12]. With InTrance, trajectories can be optimised without an initial guess starting from a broad mission description, while being applicable to a wide variety of mission scenarios [12].

To this end, the paper is structured as follows. After introducing the Alpha-Centauri binary-star system in Section 2, the dynamical framework of a one-sided and two-sided photon sail in the elliptical restricted three-body problem with two radiative sources is summarised in Section 3, based on the work in [10]. Thereafter, a mission scenario is proposed in Section 4, followed by an explanation of the optimal control problem with the associated solver for trajectory optimisation in Section 5. This leads to the discussion of the obtained results in Section 6 before concluding this paper in Section 7.

[1]Breakthrough Starshot, `https://breakthroughinitiatives.org/initiative/3` [retrieved February 11, 2021]

2 ALPHA CENTAURI

The stars Alpha Centauri A, B and C form Alpha Centauri, a triple-star system, as presented in a schematic in Fig. 1. The first two stars, hereafter referred to as α-Cen A and α-Cen B, form the binary-star system α-Cen AB. These stars are Sun-like stars, with α-Cen A being larger and more luminous, while α-Cen B is smaller and cooler than the Sun, see Table 1 that provides the radii, masses and luminosities of the three stars expressed in solar units. α-Cen C (officially termed Proxima Centauri) is the smallest and faintest of the triple-star system [1]. In its habitable zone, an Earth-sized exoplanet, Proxima Centauri b, was discovered in 2016 [13], which is the prime target of the Breakthrough Starshot project. Note that the focus of this paper is not on the scientifically interesting star α-Cen C, but rather on the binary-star system α-Cen AB. Furthermore, it is assumed that the gravitational influence and stellar radiation pressure effect of α-Cen C do not influence the photon-sail dynamics in α-Cen AB, which is justified due to the far distance between the binary-star system and α-Cen C (e.g., as a result, the radiation pressure is in the order of 10^{-17} N/m^2).

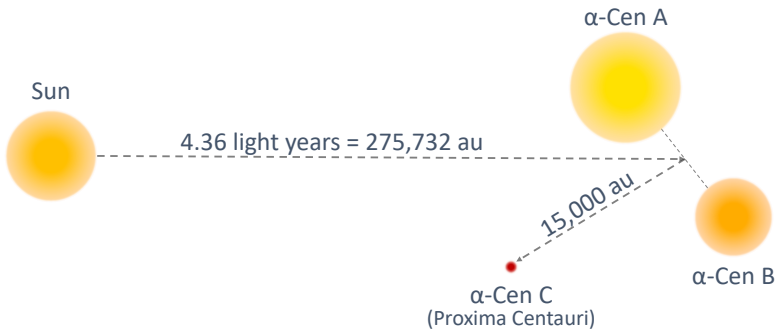

Figure 1: Schematic of the Alpha-Centauri system (distances not to scale, size of stars to scale) [10].

Table 1: Radius, mass, and luminosity of the stars of the Alpha-Centauri system.

Star	Radius, $R_\odot$	Mass, $M_\odot$	Luminosity, $L_\odot$
α-Cen A	1.2234^a	1.1055^a	1.519^b
α-Cen B	0.8632^a	0.9373^a	0.5002^b
α-Cen C	0.1542^a	0.1221^a	0.0015^c

Notes: ^{a} from [1], ^{b} from [14], ^{c} from [13].

In [10], the orbital configuration of α-Cen AB has been discussed in detail, with an explanation of the observer reference frame $\mathcal{O}_b(\hat{\mathbf{x}}_{O,b}, \hat{\mathbf{y}}_{O,b}, \hat{\mathbf{z}}_{O,b})$, which is used to describe the apparent motion of the barycentre of the binary-star system as seen from Earth. For the current paper, this apparent motion is of importance for the computation of the transfer trajectories from our planet to the α-Cen AB system. The orbits of α-Cen A and α-Cen B in frame $\mathcal{O}_b$ appear in Fig. 2. The reference frame is centred at the barycentre of α-Cen AB; the direction of $\hat{\mathbf{z}}_{O,b}$ is defined towards Earth and the plane perpendicular to $\hat{\mathbf{z}}_{O,b}$ is referred to as the "plane of the sky" or the "apparent orbital plane". The direction of $\hat{\mathbf{x}}_{O,b}$ is towards the north, while $\hat{\mathbf{y}}_{O,b}$ completes the right-handed reference frame. The figure includes the projection of the orbits of α-Cen A and B onto the plane of the sky. Hence, these projected orbits are the apparent orbits as would be observed from Earth. The semi-major axes of

the orbits of α-Cen A and B are 10.790 AU and 12.726 AU, respectively. Their smallest distance is similar to the distance between Saturn and the Sun, namely 11.3 AU, whereas their largest distance is similar to the distance between Neptune and the Sun, namely 35.8 AU. Due to conservation of angular momentum, both orbits have the same eccentricity, $e_A = e_B = e = 0.5208$, as well as the same inclination, $i_A = i_B = i = 79.320°$, which is defined as the angle from the orbital plane of α-Cen B to the plane of the sky if the observer reference frame would be centred at α-Cen A [10]. However, their argument of periapsis differs by 180°.

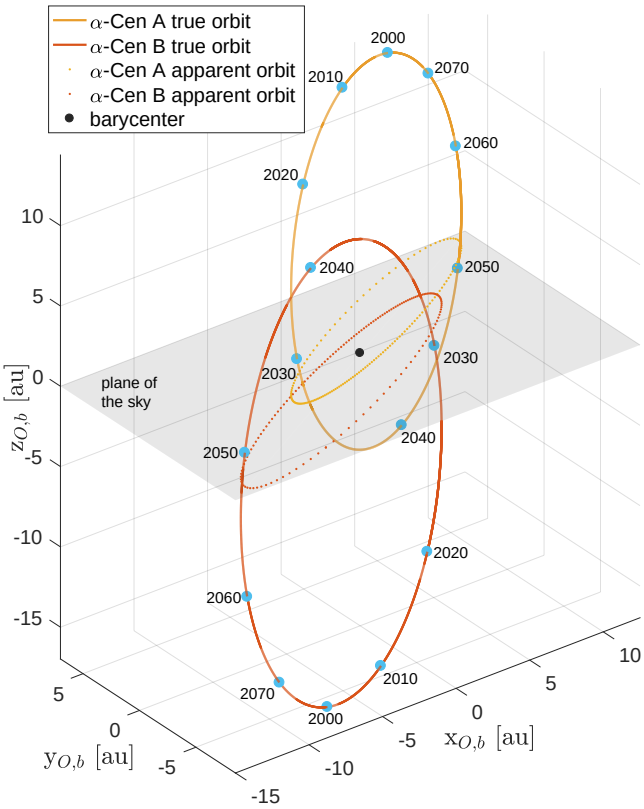

Figure 2: Orbital representations of the α-Cen AB system in frame $\mathcal{O}_b$ [10].

As this paper focuses on the photon-sail dynamics in the α-Cen AB system, it is convenient to also express the orbits of α-Cen A and B in an alternative, barycentric reference frame $\mathcal{C}(\hat{\mathbf{x}}_c, \hat{\mathbf{y}}_c, \hat{\mathbf{z}}_c)$, where $\hat{\mathbf{x}}_c$ coincides with the major axes of the orbits of both α-Cen A and B (positive towards periapsis of α-Cen B), $\hat{\mathbf{z}}_c$ points along the system's angular momentum vector and the direction of $\hat{\mathbf{y}}_c$ completes the right-handed frame, as shown in Fig. 3. The $(\hat{\mathbf{x}}_c, \hat{\mathbf{y}}_c)$-plane thus coincides with the stars' orbital plane. Hence, the inclination in frame $\mathcal{C}$ is zero degrees, while the semi-major axes and eccentricity remain unchanged. Note that the direction towards the Sun is also shown in Fig. 3, which is inclined at an angle of 10.680° with respect to the orbital plane, i.e. the complementary angle of the inclination as discussed above.

3 PHOTON-SAIL DYNAMICS

Taking into account the large eccentricity of the system, the orbital dynamics of a photon-sail spacecraft in the α-Cen AB system can be described in the photon-pressure augmented ER3BP [16]. Moreover, the dynamics for a photon sail under the effect of *two* radiative sources was derived in [10], the

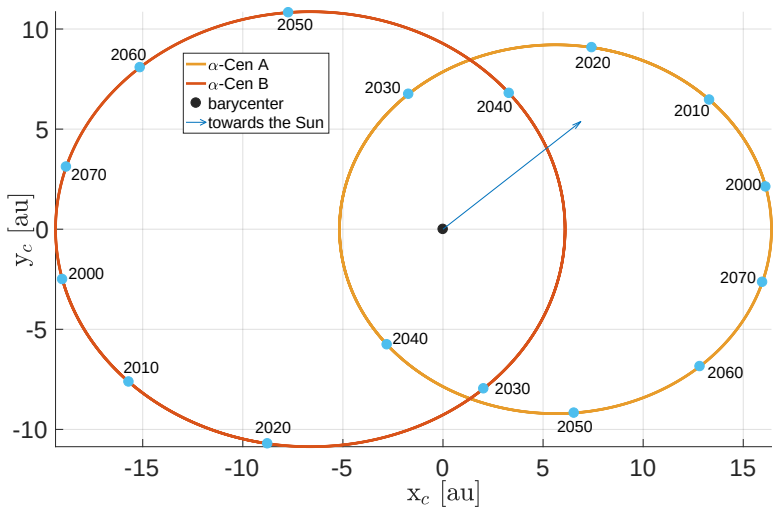

Figure 3: Orbits of α-Cen A and α-Cen B in frame $\mathcal{C}$ [15].

outcomes of which will be summarised below.

To mathematically define the photon sail's equations of motion in the ER3BP, a pulsating synodic reference frame is introduced, see Fig. 4. In frame $\mathcal{P}(\hat{\mathbf{x}}, \hat{\mathbf{y}}, \hat{\mathbf{z}})$, α-Cen A and B are stationary along the x-axis, with $\hat{\mathbf{x}}$ being the direction along the line connecting α-Cen A and B, pointing towards α-Cen B. Frame $\mathcal{P}$ rotates about the z-axis, with $\hat{\mathbf{z}}$ oriented along the angular momentum vector of the α-Cen AB system, at a non-uniform angular velocity, ω, due to the eccentricity of the orbits of the stars. The direction of $\hat{\mathbf{y}}$ completes the right-handed reference frame. The equations of motion of a photon-sail spacecraft in frame $\mathcal{P}$ can be defined as [16, 17]:

$$x'' - 2y' = \frac{1}{1 + e\cos\theta}\left(\frac{\partial U}{\partial x} + a_{s,x}\right) \tag{1}$$

$$y'' + 2x' = \frac{1}{1 + e\cos\theta}\left(\frac{\partial U}{\partial y} + a_{s,y}\right) \tag{2}$$

$$z'' + z = \frac{1}{1 + e\cos\theta}\left(\frac{\partial U}{\partial z} + a_{s,z}\right) \tag{3}$$

where differentiation occurs with respect to the true anomaly. The equations of motion are made dimensionless by using the sum of the masses of α-Cen A and B, the instantaneous distance between the two stars and the inverse of the system's mean motion as the units of mass, distance, and time, respectively. As a result, the dimensionless mass of α-Cen B is given as $\mu = \frac{M_B}{M_A + M_B} = 0.4588$ (with M_A and M_B the mass of α-Cen A and α-Cen B, respectively); one orbital period of the α-Cen AB system is represented by 2π; and the dimensionless position vectors of α-Cen A and B in frame $\mathcal{P}$ are given as $\mathbf{r}_A = [x + \mu \quad 0 \quad 0]^T$ and $\mathbf{r}_B = [x - (1 - \mu) \quad 0 \quad 0]^T$. U is the effective potential that combines the gravitational and centripetal potentials and is defined as $U = \frac{1}{2}\left(x^2 + y^2 + z^2\right) + \frac{1-\mu}{||\mathbf{r}_A||} + \frac{\mu}{||\mathbf{r}_B||}$. Finally, $\mathbf{a}_s = [a_{s,x} \quad a_{s,y} \quad a_{s,z}]^T$ is the acceleration induced by the photon sail, which is elaborated on below.

A detailed derivation of the photon-pressure acceleration in the α-Cen AB system for both a one-sided and two-sided photon sail is provided in [10], which takes into account the effect of two radiative sources on the photon-sail acceleration. The one-sided photon sail is a conventional sail, with a reflective coating on only one side of the membrane and a high-emissivity coating on the other side for

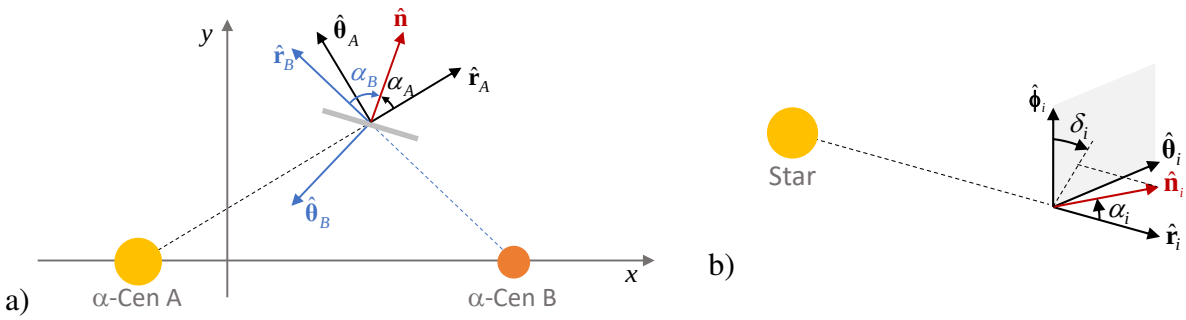

Figure 4: a) Schematic of the photon-pressure augmented ER3BP and frames $\mathcal{P}$, $\mathcal{A}$, and $\mathcal{B}$, b) definition of the cone and clock angles [10].

thermal purposes. Contrary, the two-sided photon sail is a sail configuration where both sides of the sail membrane are reflective and are allowed to be illuminated. The photon-pressure acceleration as derived in [10] makes use of the ideal reflectance model, assuming perfect specular optical properties of the sail membrane and a flat, wrinkle-free surface. As a result, the photon-pressure acceleration induced by a star will act normal to the sail surface, away from the radiating star [18]. In addition to frame $\mathcal{P}$, two additional frames ($\mathcal{A}$ and $\mathcal{B}$) are introduced in order to conveniently define the contribution of the separate stars to the total photon-sail acceleration vector. In particular, these frames are used to define the direction of the sail normal vector, the vector that is normal to the sail surface, pointing away from the star. In Fig. 4a, $\mathcal{A}(\hat{\mathbf{r}}_A, \hat{\boldsymbol{\theta}}_A, \hat{\boldsymbol{\phi}}_A)$ and $\mathcal{B}(\hat{\mathbf{r}}_B, \hat{\boldsymbol{\theta}}_B, \hat{\boldsymbol{\phi}}_B)$ are schematically presented and can be mathematically defined as:

$$\left(\hat{\mathbf{r}}_i = \frac{\mathbf{r}_i}{||\mathbf{r}_i||}, \quad \hat{\boldsymbol{\theta}}_i = \frac{\hat{\mathbf{z}} \times \hat{\mathbf{r}}_i}{||\hat{\mathbf{z}} \times \hat{\mathbf{r}}_i||}, \quad \hat{\boldsymbol{\phi}}_i = \frac{\hat{\mathbf{r}}_i \times \hat{\boldsymbol{\theta}}_i}{||\hat{\mathbf{r}}_i \times \hat{\boldsymbol{\theta}}_i||}\right), \quad i = A, B \tag{4}$$

Defining the cone angle α_i and clock angle δ_i as shown in Fig. 4b, the normal vector can be defined as:

$$\hat{\mathbf{n}}_i = \begin{pmatrix} \cos\alpha_i & \sin\alpha_i \sin\delta_i & \sin\alpha_i \cos\delta_i \end{pmatrix}^T, \quad i = A, B \tag{5}$$

In [10], the dimensionless photon-sail acceleration is defined accounting for the luminosity and mass of the stars α-Cen A and α-Cen B in the computation of the lightness number β_i (with $i = A, B$) with respect to either star. The lightness number is defined as the ratio of the stellar radiation pressure acceleration and the stellar gravitational acceleration, making it independent of the distance to the star. Note that the lightness number of a sail under effect of any of the Alpha-Centauri stars can be related to the lightness number of a sail acting in our Solar System, $\beta_\odot$, by introducing a scaling variable $\epsilon_i = \frac{L_i M_\odot}{L_\odot M_i}$, with L_i and M_i the star's luminosity and mass, respectively, as defined in Table 1. Hence, the lightness number with respect to α-Cen A and α-Cen B can be expressed as $\beta_A = \epsilon_A \beta_\odot$ and $\beta_B = \epsilon_B \beta_\odot$. Using this definition of the lightness number, the photon-sail acceleration in the α-Cen AB system for a one-sided and two-sided reflective sail can be expressed as [10]:

$$\mathbf{a}_s = \beta_\odot \left(\epsilon_A \frac{1-\mu}{||\mathbf{r}_A||^2} (\hat{\mathbf{r}}_A \cdot \hat{\mathbf{n}})^2 + u\epsilon_B \frac{\mu}{||\mathbf{r}_B||^2} (\hat{\mathbf{r}}_B \cdot \hat{\mathbf{n}})^2\right) \hat{\mathbf{n}} \tag{6}$$

with

$$\begin{aligned} u &= 1 \quad \text{if } (\hat{\mathbf{r}}_B \cdot \hat{\mathbf{n}}) \geq 0 \\ u &= -1 \quad \text{if } (\hat{\mathbf{r}}_B \cdot \hat{\mathbf{n}}) < 0 \text{ and for a two-sided reflective sail only} \end{aligned} \tag{7}$$

Note that Eq. 6 is expressed using only a reference normal vector, $\hat{\mathbf{n}}$, which is equal to the direction of the photon-sail acceleration induced by α-Cen A, i.e. $\hat{\mathbf{n}}_A$. Due to the presence of two stars, the photon sail may be illuminated on opposite sides by both stars, causing the photon-sail acceleration induced by α-Cen B to be acting in opposite direction to that induced by α-Cen A, see Fig. 5 (left) for an example. This situation is accounted for through the parameter u in Eqs. 6 and 7. However, note that, remembering the definition of a one-sided reflective sail, the situation as depicted on the left side of Fig. 5 is found to be infeasible for such a sail, as the highly emissive backside would be illuminated which would cause thermal control issues. When only one side is illuminated, the normal vectors can only be aligned, as on the right side of Fig. 5. Equation 7 includes the distinction between a one-sided and two-sided reflective sail, as the situation in the bottom row can only occur for a two-sided reflective sail. Equations 6 and 7 need to be complemented by a constraint that accounts for the fact that the photon-sail acceleration cannot be directed towards a star. This implies that $-90° \leq \alpha_A \leq 90°$, $-90° \leq \alpha_B \leq 90°$ and $-180° \leq \delta \leq 180°$, or [10]:

$$(\hat{\mathbf{r}}_A \cdot \hat{\mathbf{n}}_A) \geq 0 \quad \text{and} \quad (\hat{\mathbf{r}}_B \cdot \hat{\mathbf{n}}_B) \geq 0 \tag{8}$$

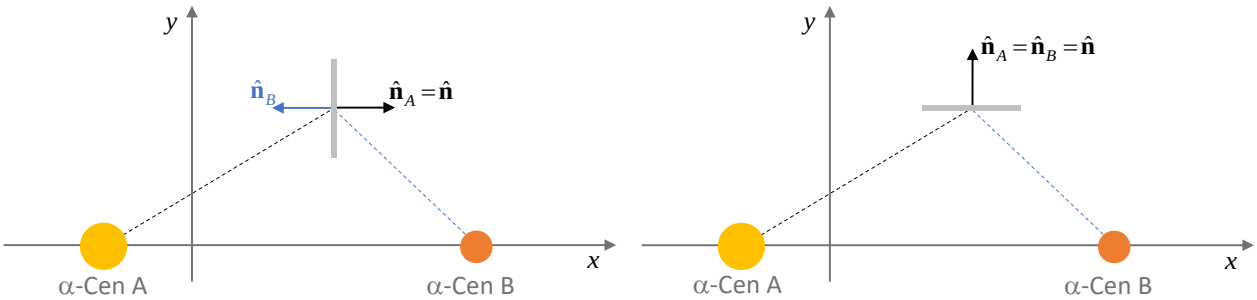

Figure 5: Orientation of normal vectors $\hat{\mathbf{n}}_A$ and $\hat{\mathbf{n}}_B$ for a two-sided reflective sail [10].

4 MISSION ANALYSIS

After introducing the Alpha Centauri system in Section 2 and presenting the dynamics for a photon sail under the effect of two radiative sources as derived in [10] in Section 3, this section discusses the mission scenario under investigation. While the inaugural mission to Alpha Centauri is presumably going to be a fly-through mission, managing a capture around one of the stars would allow a full, thorough and long-duration exploration of our neighbouring system. The following mission scenario is therefore proposed, see Fig. 6:

1) *Capture phase:* the phase which makes this mission scenario distinct from the Breakthrough Starshot proposal, designated as phase I in Fig. 6. The targeted capture orbit is a circular orbit at the centre of the habitable zone of either of the stars, which results in a circular orbit with a radius of 1.617 AU about α-Cen A and 0.967 AU about α-Cen B [19]. When orbiting one of the stars, close observations of the star and its habitable zone can be made.

2) *Transfer phase:* by transfering to the other star, this phase allows observations of both stars and their habitable zones within a single mission, see phase II in Fig. 6. The target orbit of this transfer trajectory is a circular orbit in the center of the habitable zone of the other star.

3) *Orbit-raising phase:* the final phase after arrival at the second star, see phase III in Fig. 6. The orbit altitude is raised to the outer edge of the habitable zone, either to 2.063 AU for α-Cen A or to 1.241 AU for α-Cen B [19].

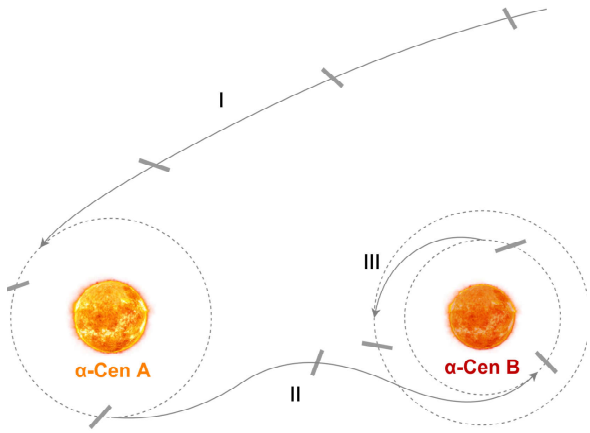

Figure 6: Graphical depiction of the mission scenario. Phase I: capture, phase II: transfer trajectory, phase III: orbit raising [15].

5 TRAJECTORY OPTIMISATION

5.1 Optimal Control Problem

As defined per the primary objective of this research, the optimal control problem is to find the optimal steering strategy, i.e. $\mathbf{u} = [\alpha\ \delta]^T$, for the photonic sail to complete the above-mentioned three-phased mission scenario and to minimise the transfer time for each of the phases while abiding by the dynamical and path constraints defined in Section 3.
It is assumed that the sail attitude can be changed instantaneously. Furthermore, a constraint on the minimum distance to both stars is enforced, to consider the limits on the temperature and integrity of the sail. The maximum temperature of the sail is set to be 373 K, so that modern silicon semiconductors still function [8]. From this maximum temperature, the minimum distance, r_{min}, can be found, which expresses the minimum distance as the minimum number of stellar radii, $\tilde{n} = \frac{r_{min}}{R_\star}$ as [8]:

$$\tilde{n} = \sqrt{\zeta}\left(\frac{\tilde{T}_\star}{\tilde{T}_{sail}}\right)^2 = 5\,(\text{for}\,\zeta = 0.05\%) \tag{9}$$

where ζ is the absorptivity of the sail and $\tilde{T}_\star$ is the temperature of the star. The temperatures of α-Cen A and α-Cen B are 5790 K and 5260 K, respectively [2]. With a reflectivity of up to 99.95%, the minimum distance is found to be five stellar radii [8].
Below, the mission phases are discussed separately to address further, phase-specific constraints and initial conditions for the optimal control problem.

5.1.1 Capture phase

The capture problem is approached as a reversed-time escape problem, where the targeted circular capture orbit at the centre of the habitable zone of one of the stars is the initial condition and the trajectory is propagated forwards in time until escape conditions while at the same time reversing the orbital motion of the binary-star system for the actual computed optimisation scenario. This approach eases the search for feasible capture trajectories as the boundary constraint of capture into a circular orbit is automatically satisfied. By propagating forwards in time starting from the escape condition

using the ordinary orbital motion of the binary-star system and using the same control vector history, the desired capture trajectory is found.
To reduce the computation time, the escape trajectory is truncated at the point along the trajectory where both the gravitational attraction and stellar radiation pressure (SRP) acceleration of α-Cen A and α-Cen B are negligibly small, i.e., smaller than 10^{-4} mm/s^2, which equals to approximately 600 AU for a graphene-like sail. In light of the mission objective to reach Alpha Centauri from our Solar System, the greatest part of the travel time occurs "after" the truncation condition is reached. Hence, the objective function J is split into two parts, as:

$$J = w_1(t_{t.c.} - t_i) + w_2(t_f - t_{t.c.})\,, \text{with}\, w_1 = 0.2\, \text{and}\, w_2 = 0.8 \tag{10}$$

where w_1 and w_2 are weights that are set based on initial test runs, such that more emphasis is put on minimising the time of flight of the interstellar part of the trajectory. Furthermore, t_i and t_f are the initial and final time of the entire trajectory, respectively, and $t_{t.c.}$ the time when the truncation condition is reached. The first part of the objective function thus covers the time of flight up to the truncation condition, while the second part accounts for the travel time from the truncation condition until our Solar System is reached. The latter is calculated analytically, by assuming that the sail's velocity at the termination condition remains constant throughout the interstellar phase of the mission. Finally, note that, although the optimal control problem is approached as an escape problem instead of a capture problem, the results are presented as a capture problem in the remaining part of this paper.

5.1.2 Transfer and orbit-raising phase

The initial condition for the last two phases of the mission scenario is assumed to be a planar circular orbit at the centre of the habitable zone, regardless of the outcome of the previous phase of the mission. The final conditions for the last two phases are defined using frame $\mathcal{C}$ in the form of a distance and velocity constraint relative to the target star (for the transfer phase) or the target orbit (for the orbit-raising phase). In particular, the final relative distance , $r_{SC}(t_f)$, and relative velocity, $\dot{r}_{SC}(t_f)$, of the spacecraft should satisfy:

$$r_{SC}(t_f) \leq \begin{cases} 1.617\,\text{AU for transfer to } \alpha\text{-Cen A} \\ 0.967\,\text{AU for transfer to } \alpha\text{-Cen B} \\ \quad 0.01\,\text{AU for orbit raising} \end{cases} \quad \text{and} \quad \dot{r}_{SC}(t_f) \leq 100\,\text{m/s} \tag{11}$$

Note that the target orbit radii for the orbit-raising phase are 2.063 AU about α-Cen A and 1.241 AU about α-Cen B.

5.2 Optimal Control Solver

All trajectories are optimised for minimum time of flight using the global low-thrust trajectory optimisation software InTrance [11, 12]. As a machine-learning approach, this software combines neural networks and evolutionary algorithms with the aim of finding (near-to) global-optimal low-thrust trajectories by optimising the thrust-vector steering strategy. To make InTrance suitable for the problem at hand, it was extended with an implementation of the dynamical model in Section 3.

6 RESULTS AND DISCUSSION

Using InTrance, the mission scenario as outlined in Section 4 is optimised. The mission scenario is simulated for four different sail materials (corresponding to four different lightness numbers to cover a wide range of sail technology levels) and two different sail configurations (the one- and two-sided

reflective sails). In Table 2, the four different sail materials are presented, in this work referred to as sail A to D, ordered by their lightness number: sail A is a Sunjammer-like sail [20], sail B is a gold-foil sail, sail C is as proposed by the Breakthrough Starshot and sail D is a graphene-class sail, which is seen as the theoretical upper limit on sail technology [7]. For each sail, the lightness number is presented with respect to the Sun as well as with respect to the two stars of Alpha Centauri, together with the corresponding sail loading.

Table 2: Sail properties used in the simulations.

Name	β			Sail Material	Sail Loading [g/m^2]
	Sun	α-Cen A	α-Cen B		
Sail A	0.040	0.057	0.023	Kapton	37
Sail B	0.765	1.055	0.422	Gold foil	2.0
Sail C	4.370	6.028	2.411	Composite Graphene-based	0.35
Sail D	1779	2453	981	Graphene	0.00086

Some final remarks with respect to the optimisation and presentation of the results are as follows:
1) Each optimisation problem is repeated at least five times, for five different seed values, to account for the inherent randomness in the evolutionary-based algorithm
2) The initial time for the optimisation of Phase I is allowed to vary within a time window of 80 years, which is equal to the orbital period of the binary-star system
3) All trajectory results will be presented in frame $\mathcal{C}$
4) The simulations are conducted for capture around α-Cen A and α-Cen B. Results are only shown for the capture trajectory that provides the shortest interstellar travel time.
5) For conciseness, only a selection of results for each of the sails specified in Table 2 will be presented.

6.1 Results for sail A

Figure 7a shows the capture trajectory into α-Cen A's centre of the habitable zone (Phase I) for a two-sided reflective "sail A"-type sail. In addition to the trajectory, the direction of the photon-sail acceleration is represented using green arrows. Note that the inset in Fig. 7a depicts a detail of the closest encounter with α-Cen A, in a new reference frame, $\mathcal{C}_{\mathcal{A}}(\hat{\mathbf{x}}_{c,a}, \hat{\mathbf{y}}_{c,a}, \hat{\mathbf{z}}_{c,a})$, which is similar to frame $\mathcal{C}$ only with the origin at the center of mass of α-Cen A. With a lightness number equal to that of sail A ($\beta_{\odot} = 0.04$), the trajectory of the sail is mainly determined by the gravitational attraction of the system, such that the trajectory follows an inwards-spiralling motion. Taking into account the earliest launch date from the year 2019, the arrival date would be in the year 20,865 after a transfer time of 18,790 years with a maximum injection speed, v_{inj}, into Alpha Centauri of 0.023% of the speed of light, c.
The time-optimal transfer trajectory from α-Cen A to α-Cen B (Phase II) of sail A is shown in Fig. 7b, with two insets showing the departure from α-Cen A and the arrival at α-Cen B (where frame $\mathcal{C}_{\mathcal{B}}(\hat{\mathbf{x}}_{c,b}, \hat{\mathbf{y}}_{c,b}, \hat{\mathbf{z}}_{c,b})$) is similar to frame $\mathcal{C}_{\mathcal{A}}$ only centered at α-Cen B). In the insets, the direction to the other stars is depicted with a red or yellow arrow. The time of flight is approximately 24 years. The sail spirals out of the centre of the habitable zone of α-Cen A and arrives in the habitable zone of α-Cen B when α-Cen B is close to its periapsis in its orbit around α-Cen A.

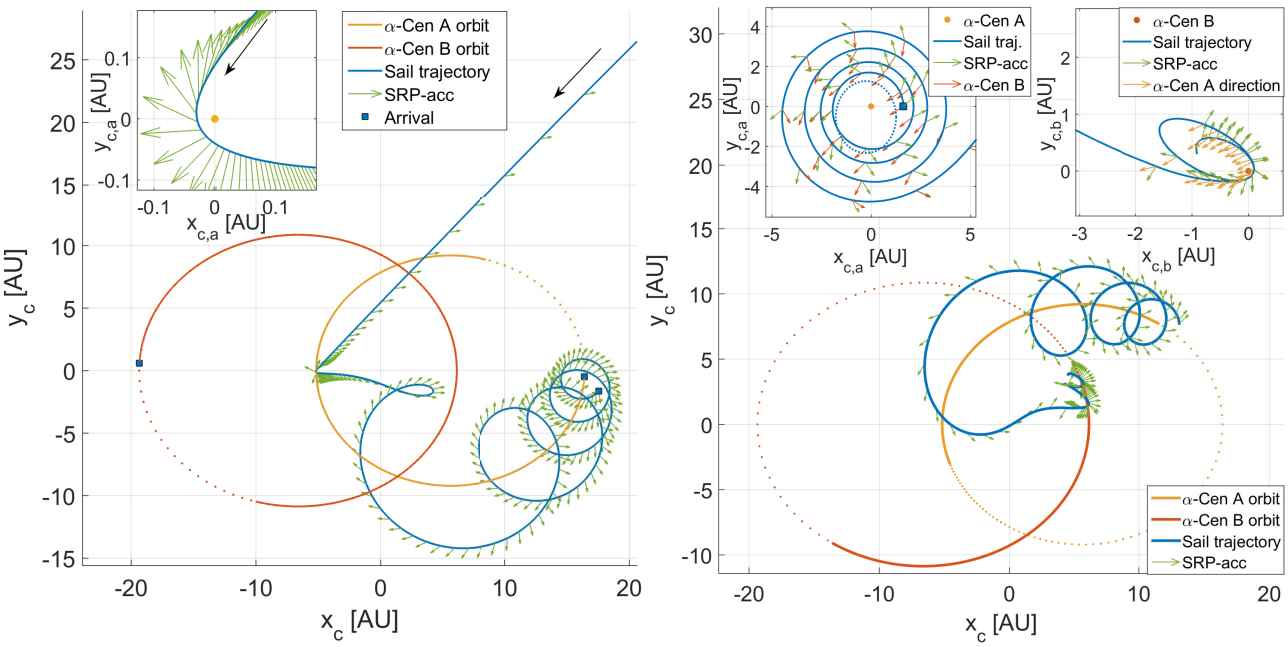

(a) (b)

Figure 7: Sail A: a) Phase I capture trajectory, b) Phase II transfer trajectory from α-Cen A to α-Cen B [15].

6.2 Results for sail C

To compare the performance of a one-sided and two-sided reflective sail, capture trajectories for both sail configurations are presented in Fig. 8 for sail C.
The time-optimal capture trajectory for a one-sided "Sail C"-type sail, see Fig. 8a, arrives at α-Cen A with a time of flight of 16,372 years and an injection speed of 0.026% of the speed of light. Although it is in theory possible, it is found to be practically unfeasible to travel from our Solar System to Alpha Centauri with a one-sided reflective sail due to the significant constraint that the one-sidedness imposes on the trajectory, as similar results were found for the other sail materials.
For the two-sided reflective sail, the optimised trajectory exploits a "reversed-photogravitational assist" about α-Cen A, where the sail travels straight towards the star and uses the sail not to gain energy (as would be the case for a traditional photogravitational assist), but to maximise its deceleration before capture into an orbit around α-Cen B. To arrive at α-Cen B, this mission would take approximately 2,000 years with an injection speed of 0.23% of the speed of light and the earliest arrival date would be the year 3987.

6.3 Results for sail D

The capture trajectory of the two-sided reflective sail with the most optimistic lightness number, sail D, is shown in Fig. 9. As for sail C, a "reversed-photogravitational assist" is performed at α-Cen A, which is in line with the results found in [7, 8]. Note that, in Fig. 9b, the scale in z_c-direction is different from those in x_c- and y_c-direction to amplify the out-of-plane motion. With this sail, the arrival date would be in the year 2172 after travelling for 111 years, which is a significant improvement from sail C in terms of travel time. Note that the departure in the Solar System would be in the year 2060 to ensure the arrival conditions in Alpha Centauri as depicted in Fig. 9. The sail would enter

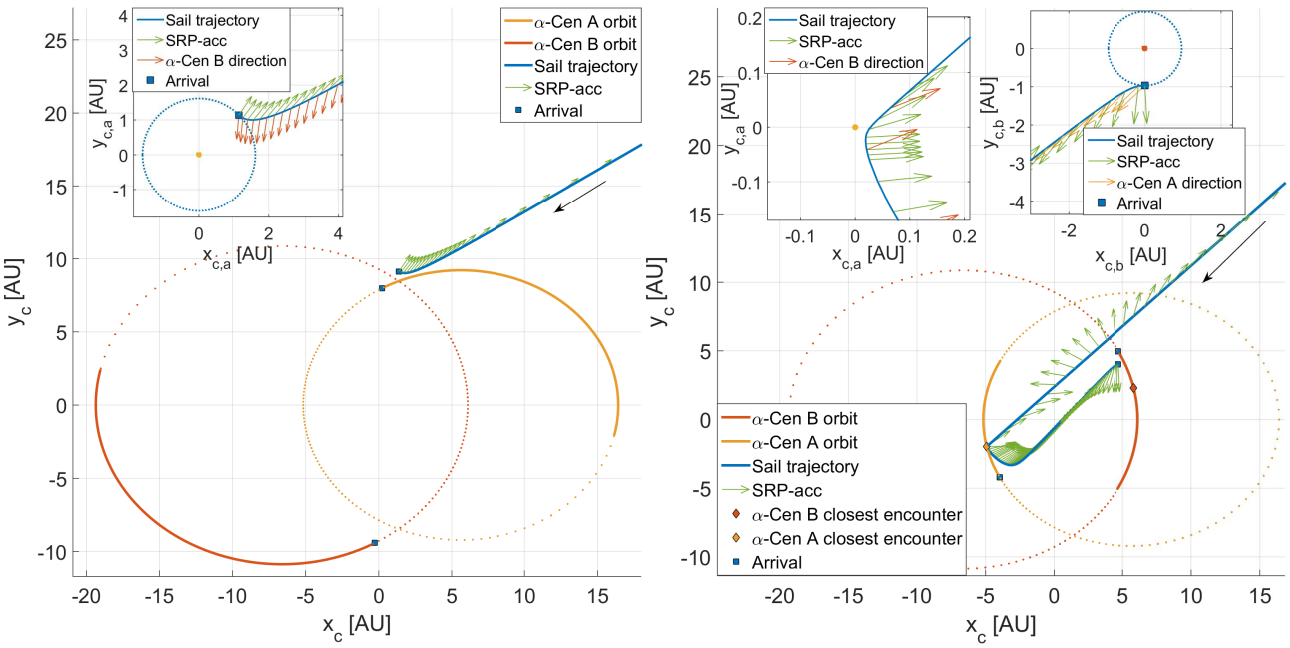

(a) (b)

Figure 8: Sail C: a) Phase I capture trajectory for a one-sided reflective sail, b) Phase I capture trajectory for a two-sided reflective sail [15].

Alpha Centauri with a speed of 3.9% of the speed of light, corresponding to 6.75 AU per day.
While the results for capture with this sail show promising trajectories, it is found to be challenging to obtain results for the two remaining phases of the mission. Therefore, it is suggested to jettison the sail after the capture phase, such that the mission ends in an orbit about α-Cen A.
To investigate whether the travel time could be reduced even further by loosening the constraint on capture into a circular orbit, additional simulations have been run with non-circular arrival orbits after capture. By changing the arrival conditions at α-Cen B from a circular orbit to a highly eccentric orbit ($ecc = 0.9$), the travel time from our Solar System to an orbit about α-Cen B decreases to 77.6 years, with an injection speed of approximately 5.5% of the speed of light, corresponding to approximately 9.5 AU per day.

6.4 Overview of the results

The results for the four sail configurations and for the three phases of the proposed mission scenario are summarised in Table 3. The results presented in this work show an average improvement of 30% in terms of time of flight compared to previous work [7]. It is important to note that the two-sided reflective case for sail A shows a similar performance as that for the one-sided reflective case for sail C. This result suggests that it is worth performing research and development of two-sided reflective sail technology.

7 CONCLUSION

This work investigated the orbital dynamics of a photon sail in the Alpha-Centauri binary system as well as time-optimal trajectories from our Solar System to Alpha Centauri, which is seen as the prime target of interstellar travel. Contrary to the proposal of the Breakthrough Starshot project to fly

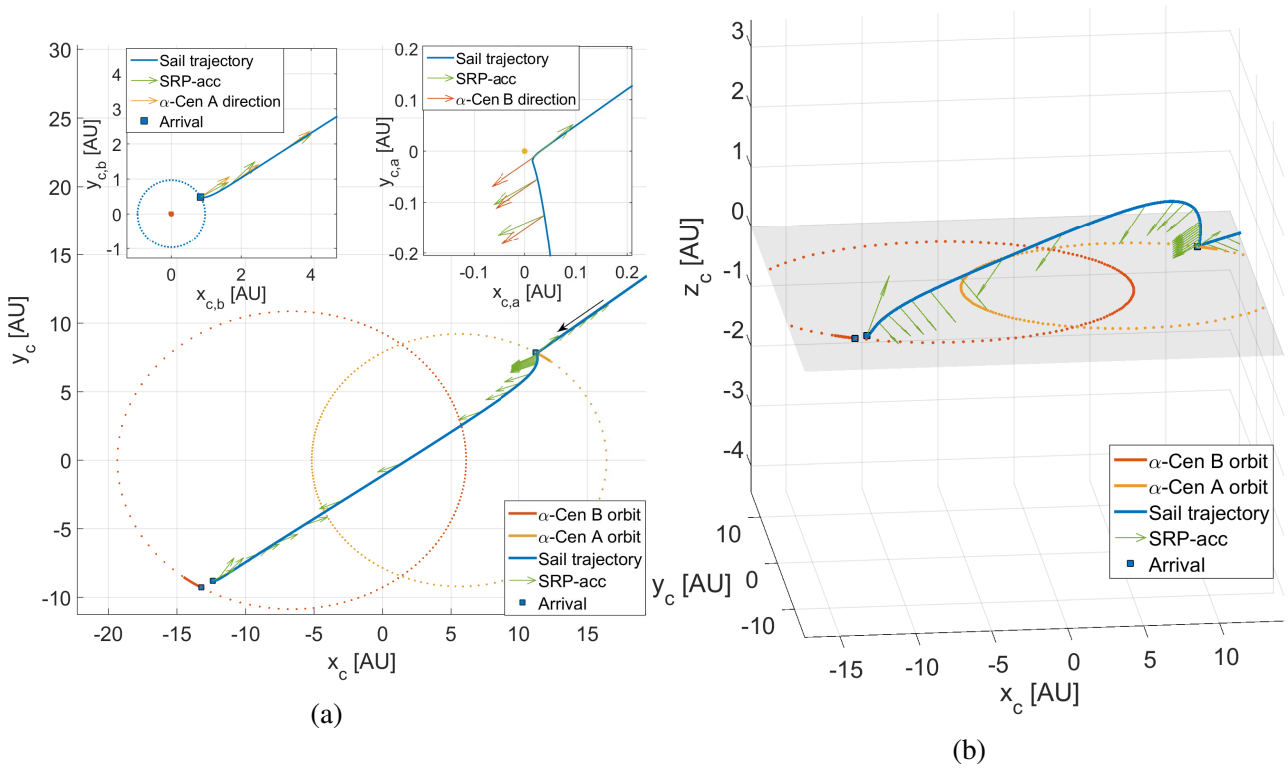

Figure 9: Sail D: a) Phase I capture trajectory, b) Phase I capture trajectory in 3D [15].

Table 3: Overview of all results [15].

Sail	Configuration	Injection speed [% c]	Time of flight (yrs) Capture	Transfer	Orbit raising
Sail A	two-sided reflective	0.02	18,790	23.8	3.0
Sail B	two-sided reflective	0.19	2,293	5.4	1.0
Sail C	two-sided reflective	0.23	1,950	2.3	1.8
	one-sided reflective	0.03	16,372	18.3	2.7
Sail D	two-sided reflective	3.90	111	0.3	n.a.
	idem, $ecc = 0.9$	5.50	77.6	n.a.	n.a.

through Alpha Centauri, this research focused on capture into the Alpha-Centauri system to increase the scientific yield of the mission. After showing the feasibility of the sail being captured into a bound orbit about one of the stars, more mission applications were examined, in particular: transfer trajectories to the other star and orbit raising about the star. These capture, transfer and orbit-raising trajectories were optimised using an adapted version of InTrance, a trajectory optimisation software combining artificial neural networks and evolutionary algorithms, for a range of sail performance levels representative of near- to future-term photon-sail technology and for two sail configurations: a one-sided reflective photon sail and a two-sided reflective photon sail. The conclusions drawn from the results can be summarised as follows:

1) For present-day solar-sail technology, i.e. a Sunjammer-like sail [20], the spacecraft would need approximately 20,000 years to arrive and be captured into the Alpha-Centauri binary system. Therefore, sending a sail today would presumably mean that it would be overtaken by a more advanced photonic sail launched in the future;
2) The Breakthrough Starshot project, with its proposal of a fly-through mission, aims at travelling to Alpha Centauri within 20 years. When considering capture into the binary-star system for a sail performance equal to that proposed by the Breakthrough Starshot project, this travel time increases to approximately 2,000 years;
3) A futuristic ultralight sail could enable a transfer from Earth and capture into an orbit about Alpha Centauri B within less than 80 years. However, it is found to be extremely challenging for such a high-tech sail to perform transfer trajectories or orbit-raising manoeuvres once inside the Alpha-Centauri system. Therefore, it is suggested to jettison the sail upon arrival and remain bounded to Alpha Centauri B;
4) Although it is possible to be captured in the Alpha-Centauri system using a sail that is reflective on one side only, the interstellar travel time could be reduced by a factor of eight using a sail that is reflective on both sides. However, such a two-sided reflective sail would require significant innovations with respect to current sail technology, particularly regarding the thermal control of the sail membrane.
The capture trajectories obtained in this work show an average improvement of 30% in terms of interstellar flight time compared to previous work [7]. Still, significant technological development is required to reach and be captured in the Alpha-Centauri system in less than a century. Therefore, a fly-through mission arguably remains the only option for a first mission to Alpha Centauri, but the enticing results obtained in this work provide perspective for future long-residence missions to our closest neighbouring star system.

REFERENCES

[1] P. Kervella, F. Thévenin, and C. Lovis, "Proxima's orbit around α Centauri," *Astronomy and Astrophysics*, vol. 598, no. L7, 2017.

[2] T. Pino and C. Circi, "A star-photon sailcraft mission in the Alpha Centauri system," *Advances in Space Research*, vol. 59, pp. 2389 – 2397, 2017.

[3] Y. Tsuda, O. Mori, R. Funase, H. Sawada, T. Yamamoto, T. Saiki, T. Endo, and J. Kawaguchi, "Flight status of IKAROS deep space solar sail demonstrator," *Acta Astronautica*, vol. 69, no. 9–10, pp. 833 – 840, 2011.

[4] L. Johnson, M. Whorton, A. Heaton, R. Pinson, G. Laue, and C. Adams, "NanoSail-D: A solar sail demonstration mission," *Acta Astronautica*, vol. 68, no. 5–6, pp. 571 – 575, 2011.

[5] R. W. Ridenoure, R. Munakata, S. D. Wong, A. Diaz, D. A. Spencer, D. A. Stetson, B. Betts, B. A. Plante, J. D. Foley, and J. M. Bellardo, "Testing the LightSail program: Advancing solar sailing technology using a CubeSat platform," *Journal of Small Satellites*, vol. 5, no. 2, pp. 531 – 550, 2016.

[6] B. Betts, D. Spencer, B. Nye, R. Munakata, J. Bellardo, S. Wong, A. Diaz, R. Ridenoure, B. Plante, J. Foley, and J. Vaughn, "LightSail 2: Controlled solar sailing using a Cubesat," in *Fourth International Symposium on Solar Sailing 2017*, Kyoto, Japan, 2017, p. 7.

[7] R. Heller and M. Hippke, "Deceleration of high-velocity interstellar photon sails into bound orbits at α Centauri," *The Astrophysical Journal Letters*, vol. 835, no. L32, 2017.

[8] R. Heller, M. Hippke, and P. Kervella, "Optimized trajectories to the nearest stars using lightweight high-velocity photon sails," *The Astronomical Journal*, vol. 154, no. 115, 2017.

[9] G. Aliasi, G. Mengali, and A. A. Quarta, "Artificial equilibrium points for a solar balloon in the α Centauri system," *Acta Astronautica*, vol. 104, no. 2, pp. 464 – 471, 2014.

[10] J. Heiligers, F. Schoutetens, and B. Dachwald, "Photon-sail equilibria in the Alpha Centauri system," *Journal of Guidance, Control, and Dynamics*, vol. 44, no. 5, pp. 1053–1061, 2021.

[11] B. Dachwald, "Low-thrust trajectory optimization and interplanetary mission analysis using evolutionary neurocontrol," Ph.D. thesis, Universität der Bundeswehr München, 2004.

[12] A. Ohndorf, "Multiphase low-thrust trajectory optimization using evolutionary neurocontrol," Ph.D. thesis, Delft University of Technology, 2016.

[13] Anglada-Escudé, G., Amado, P. J., Barnes, J., Berdiñas, Zaira M., Butler, R. Paul, Coleman, Gavin A. L., de la Cueva, Ignacio, Dreizler, Stefan, Endl, Michael, Giesers, Benjamin, Jeffers, Sandra V., Jenkins, James S., Jones, Hugh R. A., Kiraga, Marcin, Kürster, Martin, López-González, María J., Marvin, Christopher J., Morales, Nicolás, Morin, Julien, Nelson, Richard P., Ortiz, José L., Ofir, Aviv, Paardekooper, Sijme-Jan, Reiners, Ansgar, Rodríguez, Eloy, Rodríguez-López, Cristina, Sarmiento, Luis F., Strachan, John P., Tsapras, Yiannis, Tuomi, Mikko, and Zechmeister, Mathias, "A terrestrial planet candidate in a temperate orbit around Proxima Centauri," *Nature*, vol. 536, pp. 437–440, 2016.

[14] Thévenin, F., Provost, J., Morel, P., Berthomieu, G., Bouchy, F., and Carrier, F., "Asteroseismology and calibration of α Cen binary system," *Astronomy and Astrophysics*, vol. 392, no. 1, pp. L9–L12, 2002.

[15] F. Schoutetens, "Photon-sail trajectory optimization in Alpha Centauri using evolutionary neurocontrol," MSc thesis, Delft University of Technology, 2019.

[16] V. Szebehely, *Theory of Orbits: The Restricted Problem of Three Bodies*. Academic Press, 1967.

[17] H. Baoyin and C. R. McInnes, "Solar sail equilibria in the elliptical restricted three-body problem," *Journal of Guidance, Control and Dynamics*, vol. 29, no. 3, pp. 538–543, 2006.

[18] C. R. McInnes, *Solar Sailing: Technology, Dynamics and Mission Applications*. Berlin, Germany: Springer - Praxis Books in Astronautical Engineering, Springer-Verlag, 1999, pp. 1, 214–224.

[19] R. K. Kopparapu, R. M. Ramirez, J. SchottelKotte, J. F. Kasting, S. Domagal-Goldman, and V. Eymet, "Habitable Zones around Main-sequence Stars: Dependence on Planetary Mass," *The Astrophysical Journal*, vol. 787, no. 2, p. L29, 2014.

[20] J. Heiligers, B. Diedrich, W. Derbes, and C. McInnes, "Sunjammer: Preliminary end-to-end mission design," in *AIAA/AAS Astrodynamics Specialist Conference*, San Diego, California, USA, 2014, p. 27.